

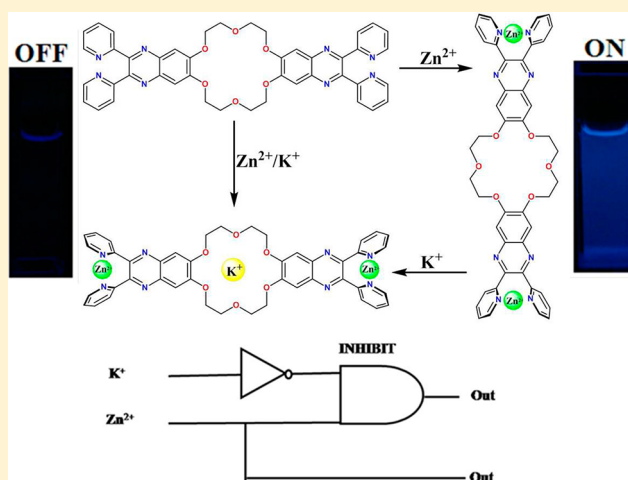
Ratiometric and Selective Fluorescent Sensor for Zn^{2+} as an “Off–On–Off” Switch and Logic Gate

Ya-Ping Li, Hua-Rong Yang, Qiang Zhao, Wei-Chao Song, Jie Han, and Xian-He Bu*

Tianjin Key Lab on Metal and Molecule-based Material Chemistry, Department of Chemistry, Nankai University, Tianjin 300071, China

Supporting Information

ABSTRACT: A new chemosensor, 2,3,15,16-tetrakis(pyridin-2-yl)-7,8,10,11,20,21,23,24-octahydro[1,4,7,10,13,16]-hexaoxacyclooctadecino[2,3-g:11,12-g']diquinoxaline (**1**), containing 2,3-bis(pyridin-2-yl)quinoxaline and crown ether moieties, has been designed and found to be a ratiometric and selective fluorescent detector of Zn^{2+} over a wide range of tested metal ions. The addition of Zn^{2+} to the solution of **1** in acetonitrile induced the formation of a 1:2 ligand–metal complex, 1-Zn^{2+} , which exhibits a remarkable enhanced fluorescent emission centered at 460 nm, with the disappearance of the fluorescent emission of **1** centered at 396 nm due to the mechanism of internal charge transfer. In contrast, the presence of K^+ results in the fluorescence quenching of **1** and 1-Zn^{2+} through the photoinduced electron-transfer mechanism. These results demonstrate that **1** can perform as not only an INHIBIT logic gate but also an “off–on–off” molecular switch triggered by Zn^{2+} and K^+ . The structure of complex 1-Zn^{2+} has been characterized by single-crystal X-ray crystallography, mass spectrometry, and ^1H NMR titration experiments. Density functional theory calculation results on **1** and the 1-Zn^{2+} complex are well consistent with the experimental results.



INTRODUCTION

Recently, much attention has been focused on the development of a ratiometric and fluorescent probe for zinc ions in supramolecular chemistry.¹ As is well-known, Zn^{2+} plays an important role in the human body and in biological activities such as structural and catalytic cofactors, neural signal transmitters, or modulators.² The development of highly selective and ratiometric fluorescent chemosensors for Zn^{2+} ions is still an important task,³ although some fluorescent sensors for Zn^{2+} by the ratio of the emission intensity changes at two wavelengths have been reported in the literature.^{3a,j–n} Especially, ratiometric fluorescent probes are more favored by the researchers because a ratiometric read-out eliminates the environmental influence on the fluorescence intensity.

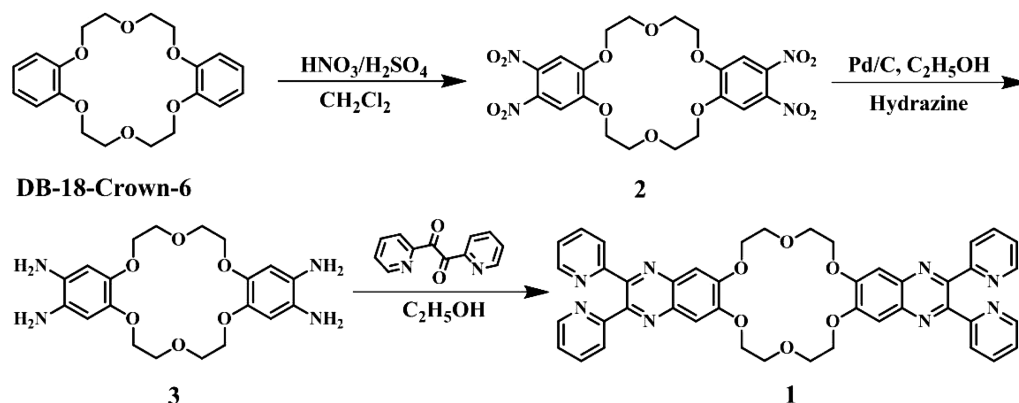
A number of fluorescent sensors/probes have been reported as molecular logic gates.^{4,5} In general, the reported systems were devised by modulation of the emission properties of the sensors by different combinations of heavy-metal ions, such as Hg^{2+} and Cd^{2+} .⁶ It is still a challenge to develop a fluorescent sensor with different metal-chelating ability and chelating modes, which make its emission state modulated conveniently to create logic gates.⁷ From a literature search, the molecular logic gates and/or switches on a single fluorescent sensor by K^+ and Zn^{2+} ions are still limited.⁸ In this regard, it is important

and interesting to seek a fluorescent sensor to construct logic gates and switches with Zn^{2+} and K^+ .

Until now, di-2-picolyamine, cyclic polyamines, and acyclic iminodiacetic acid, bipyridine, quinoline, and Schiff bases have been used as Zn^{2+} chelators;^{3j,9} they all have a defined coordination pattern and show strong affinities to Zn^{2+} . In contrast, crown ether units have been proven to exhibit excellent binding ability with alkali metals; among many kinds of crown ethers, [2,4]dibenzo-18-crown-6 derivatives and calixcrowns have great preference for K^+ ions.^{8,10,11} Herein, we present a new fluorophore, 2,3,15,16-tetrakis(pyridin-2-yl)-7,8,10,11,20,21,23,24-octahydro[1,4,7,10,13,16]-hexaoxacyclooctadecino[2,3-g:11,12-g']diquinoxaline (**1**), which consists of two different binding moieties [2,3-bis(pyridin-2-yl)quinoxaline and [2,4]dibenzo-18-crown-6]. 2,3-Bis(pyridin-2-yl)quinoxaline was chosen as a building block because of its affinity for Zn^{2+} and/or Cd^{2+} ions as well as its excellent optical properties and extensive application in molecular sensory systems as a signaling component.¹² We found that **1** shows ratiometric and selective fluorescent recognition of Zn^{2+} ions through the mechanism of internal charge transfer (ICT),⁹ and the recognition behavior can be

Received: April 10, 2012

Scheme 1



modulated by K^+ through the photoinduced electron-transfer (PET) mechanism.¹¹ As a result, **1** can be used as a novel INHIBIT logic gate and an “off–on–off” molecular switch triggered by Zn^{2+} and K^+ .

EXPERIMENTAL SECTION

Materials and General Methods. All of the starting materials for synthesis were commercially available and were used as received. All of the solvents used for titration measurements were purified by standard procedures. ^1H NMR spectra were measured in CDCl_3 at 25 °C, and ^1H NMR titration was measured in CDCl_3 /dimethyl sulfoxide ($\text{DMSO}-d_6$) with Varian Unity Plus 400 MHz NMR spectrometer (Varian, USA). Elemental analyses (C, H, and N) were performed on a Perkin-Elmer 240C analyzer (Perkin-Elmer, USA). IR spectra were measured on a TENSOR 27 OPUS FT-IR spectrometer with KBr pellets in the range 4000–400 cm^{-1} (Bruker, Germany). UV–vis absorption spectra were measured with a Hitachi U-3010 UV–vis spectrophotometer (Hitachi, Japan). Fluorescence spectra were recorded at room temperature on a Varian Cary Eclipse fluorescence spectrometer (Varian, USA).

Preparation of Solutions for Fluorometric and UV–Vis Titration. Cations (K^+ , Na^+ , Ca^{2+} , NH_4^+ , Mg^{2+} , Mn^{2+} , Fe^{3+} , Ni^{2+} , Co^{2+} , Cu^{2+} , Cu^+ , Ag^+ , Hg^{2+} , Cd^{2+} , Zn^{2+} , Eu^{3+} , and Sr^{2+}) of 0.01 M in acetonitrile were prepared. The concentration of **1** in fluorescence titration tests was 50 μM with CH_3CN as the solvent. The UV–vis titration concentration of **1** was studied in a CH_3CN solution with 5 μM . During titration, metal ions were added using the microinjector to a solution of **1** (2.5 mL), and the whole volume of **1** and metal ions could be considered as 2.5 mL because the volume of metal ions could be ignored compared to that of **1**. After stirring, the fluorescence spectra were recorded. For all measurements, excitation and emission slit widths were 5 nm.

Synthesis of Fluorophore 1. As shown in Scheme 1, the intermediate compound **3**¹³ (210 mg, 0.5 mmol), 1,2-bis(pyridin-2-yl)ethane-1,2-dione (212 mg, 1 mmol), and a few drops of acetic acid as catalysts were dissolved in ethanol (20 mL) under a nitrogen atmosphere, and the mixture was heated under reflux for ca. 4 h. The reaction mixture was cooled and filtered to afford the crude product, which was purified by recrystallization from $\text{C}_2\text{H}_5\text{OH}$ to give 126 mg (30%) of **1** as slight-yellow solid. ESI-MS: m/z 773.2 ($[\text{M} + \text{H}]^+$). Anal. Calcd for $\text{C}_{44}\text{H}_{36}\text{N}_8\text{O}_6$: C, 68.38; H, 4.70; N, 14.50. Found: C, 68.23; H, 4.59; N, 14.42. ^1H NMR (CDCl_3 - d_6 , 400 MHz): δ 8.56 (m, 4H), 7.76 (m, 8H), 7.45 (s, 4 H), 7.39 (s, 4H, quinoxaline phenyl proton), 4.37 (dd, $J = 3.5$ and 1.6 Hz, 8H), 4.13 (d, $J = 2.2$ Hz, 8H). IR (KBr pellet, cm^{-1}): ν_{max} 1693, 1653, 1559, 1541, 1457, 1389. This compound was further characterized by X-ray diffraction analysis (see Figure S1 in the Supporting Information).

Synthesis of 1-Zn. In a tube, a mixture of 1:1 (v/v) CH_2Cl_2 / CH_3CN (10 mL) was carefully layered over a CH_2Cl_2 (3 mL) solution of **1** (0.05 mmol) as a buffer layer, over which a solution of ZnCl_2 (0.15 mmol) in CH_3CN (3 mL) was carefully added, and the resultant

system was left undisturbed at room temperature. Brown block-shaped crystals of **1-Zn** were obtained after about 3 weeks. FT-IR (KBr pellets, cm^{-1}): 3447, 2925, 1622, 1559, 1490, 1447, 1363, 1340, 1264, 1223, 1135, 1054, 954, 779, 699. Anal. Calcd for $\text{C}_{50}\text{H}_{50}\text{Zn}_2\text{N}_{10}\text{O}_8\text{Cl}_4$: C, 50.40; H, 4.23; N, 11.75. Found: C, 50.64; H, 4.46; N, 11.39.

X-ray Data Collection and Structure Determinations. Single-crystal X-ray diffraction data for **1** was collected on a SCX-Mini diffractometer at 293 K, and those for complex **1-Zn** were collected on a Rigaku RAXIS-RAPID diffractometer at 273 K with Mo $K\alpha$ radiation ($\lambda = 0.71073$ Å) by ω scan mode. The program SAINT¹⁴ was used for integration of the diffraction profiles. All of the structures were solved by direct methods using the SHELXS program of the SHELXTL package and refined by full-matrix least-squares methods with SHELXL (semiempirical absorption corrections were applied using the SADABS program).¹⁵ Metal atoms in complex **1-Zn** were located from E maps, and other non-H atoms were located in successive difference Fourier syntheses and refined with anisotropic thermal parameters on F^2 . The H atoms of the ligands were generated theoretically onto the specific atoms and refined isotropically with fixed thermal factors. Detailed crystallographic data are summarized in Table S1 and the selected bond lengths and angles of **1** and **1-Zn**²⁺ are given in Tables S2 and S3 in the Supporting Information.

Theoretical Calculations. Theoretical investigations on **1** and **1-Zn** were performed by the Gaussian03 program package¹⁶ method. The geometrical structures of **1** and **1-Zn** were fully optimized. The optimized structure of the **1-Zn** complex was very close to its single-crystal X-ray diffraction structure.

RESULTS AND DISCUSSION

Absorbance and Fluorescence. The binding properties of **1** with different kinds of cations (K^+ , Na^+ , Ca^{2+} , Mg^{2+} , Sr^{2+} , Eu^{3+} , Cu^{2+} , Cu^+ , Ni^{2+} , Fe^{3+} , Co^{2+} , Hg^{2+} , Mn^{2+} , Nd^{3+} , NH_4^+ , Cd^{2+} , Ag^+ , and Zn^{2+}) were investigated by UV–vis absorption and fluorescence emission spectra. With an excitation wavelength at 320 nm, **1** (50 μM) showed a strong emission peak at 396 nm, and the addition of Cu^{2+} , Cu^+ , Ni^{2+} , Fe^{3+} , Co^{2+} , Hg^{2+} , Mn^{2+} , and Ag^+ ions induced the fluorescence quenching of **1**, whereas very weak variations were observed upon the addition of an excess of K^+ , Na^+ , Ca^{2+} , Mg^{2+} , Sr^{2+} , Eu^{3+} , Nd^{3+} , and NH_4^+ cations, which show strong binding affinity with [2,4]dibenzo-18-crown-6.¹⁷ Only the addition of Zn^{2+} to the solution of **1** resulted in a prominent red shift of the fluorescence maximum of about 64 nm from 396 to 460 nm (see Figure S2 in the Supporting Information). Meanwhile, the ratio of the emission intensities at 396 and 460 nm (I_{460}/I_{396}) changed from 0.09 to 293.84 upon the addition of Zn^{2+} . The fluorescence quantum yield of **1** is 0.36 but increased to 0.75 upon Zn^{2+} addition.¹⁸ The results indicated that **1** can serve as a ratiometric fluorescent sensor for Zn^{2+} .

The selectivity of the fluorescent response of **1** (50 μM) to zinc ions was then examined in a CH_3CN solution (see Figure 1). After Zn^{2+} ions were added to the solution of **1**, the

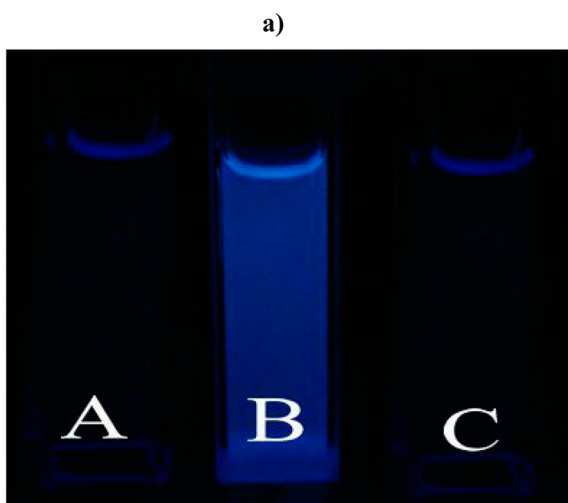
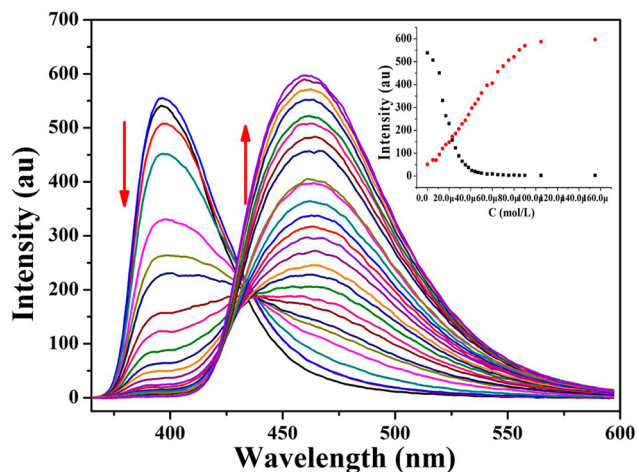


Figure 1. (a) Fluorescence spectra ($\lambda_{\text{ex}} = 320 \text{ nm}$) of **1** (50 μM) in the presence of different concentrations of Zn^{2+} (0–2 equiv) in CH_3CN (2.5 mL). Both the excitation and emission slit widths were 5 nm. Inset: Ratiometric combinational curve I_{460} (red) and I_{396} (black) as a function of $[\text{Zn}^{2+}]$ increased. (b) Visible emission observed from samples of **1**, **1**- Zn^{2+} , and **1** with other metal ions under a hand-held UV-vis (365 nm) lamp: (A) only **1**; (B) **1**- Zn^{2+} ; (C) **1** with other metal ions.

fluorescence intensity at 396 nm was gradually decreased, whereas the intensity at 460 nm gradually increased and reached a plateau after 2 equiv of Zn^{2+} was added; meanwhile, a new isoemissive point at 428 nm appeared, implying the formation of a well-defined complex between Zn^{2+} and **1**. The solution of **1** with 2 equiv of Zn^{2+} ions converted the visual emission color from dark to blue when excited with a hand-held 365 nm UV lamp (Figure 1b). The red shift in the emission of **1** after Zn^{2+} coordination can be explained in terms of the ICT mechanism.^{3i,12} In general, a significant number of ICT-based ratiometric fluorescence probes show broad fluorescence spectra before and after binding target ions and have a high degree of overlap (in some cases, the spectra with lower

intensity can be completely covered by the broad one with high intensity), which makes it difficult to accurately determine the ratio of the two fluorescence peaks. As a result, it is usually impossible to quantitatively analyze the target ions. However, the two emission bands of **1** before and after binding Zn^{2+} have a low degree of overlap, and thus the ratio of the two fluorescence peaks at 396 and 460 nm, respectively, can be well determined. These data establish that **1** functions as a single-excitation, dual-emission ratiometric probe for Zn^{2+} .

When the cation metal interacts with the acceptor group, the excited state is more stabilized by the cation than is the ground state, and this leads to a red shift of the absorption and emission spectra.^{4e,9a,12} This mechanism is quite general, and the experimental observations have been confirmed by the density functional theory (DFT) calculation results, which will be discussed later in this paper.

In addition, further investigation was carried out on the changes of UV-vis spectra upon the addition of Zn^{2+} ions to the CH_3CN solution of **1** (5 μM ; see Figure 2). With increasing

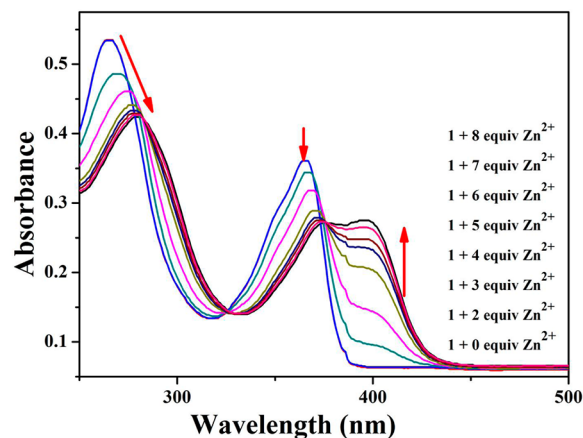


Figure 2. Absorption spectra of **1** (5 μM) in the presence of different concentrations of Zn^{2+} (0–8 equiv) in CH_3CN .

concentration of Zn^{2+} ions (0–8 equiv), the absorption peak at 365 nm was gradually decreased and a new peak at 396 nm appeared simultaneously (red shift), accompanying the appearance of two well-defined isosbestic points at 426 and 375 nm, indicating new species formed between **1** and Zn^{2+} ions. The interactions between **1** and zinc ions were also studied by ^1H NMR spectroscopy in a $\text{DMSO}-d_6/\text{CDCl}_3$ solution. Upon the addition of Zn^{2+} ions to the solution of **1**, the chemical shift of the pyridyl protons of **1** at 8.56 ppm moves to 8.49 ppm, suggesting that coordination of Zn^{2+} to the pyridyl N atom occurred^{6a} (see Figure S3 in the Supporting Information). The coordination mode of Zn^{2+} to **1** has been characterized by single-crystal X-ray diffraction, which will be described later in this paper.

A nonlinear fitting procedure of fluorescence titrations revealed that **1** coordinates with Zn^{2+} in a 1:2 stoichiometry, and the binding constant is $\log \beta_2 = 9.83 \pm 0.04$ (see Figure S4a in the Supporting Information).¹⁹ The Job's plot also suggests that **1** formed the 1:2 complex with Zn^{2+} (see Figure S4b in the Supporting Information). Furthermore, the electrospray ionization mass spectrometry (ESI-MS) spectrum of the complex cation displays peaks at m/z 900.4 (calcd m/z 900.4) for $[\text{1-2Zn}^{2+}]$ in acetonitrile, which also confirms the

formation of 1-Zn²⁺ (see Figure S5 in the Supporting Information).

Selection and Competition Experiments. A series of interference experiments demonstrated that the presence of other tested metal cations could hardly disturb 1 in recognizing the Zn²⁺ ion except for the K⁺ ion (see Figures 3a and S6a in

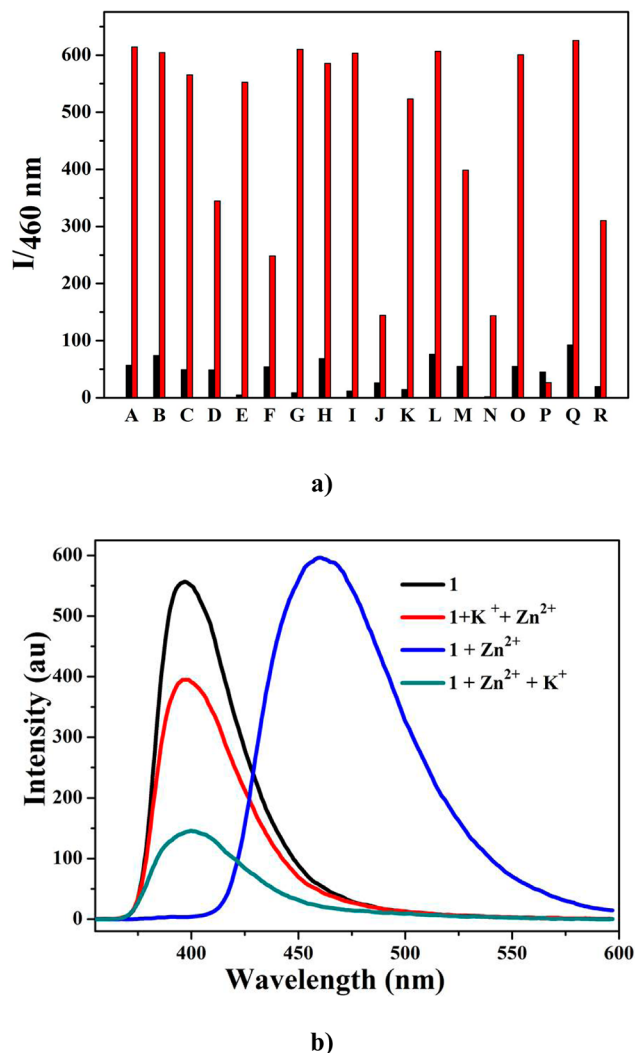


Figure 3. (a) Analysis of the maximum fluorescence intensity ratio at 460 nm of 1 (50 μM) and 1-Zn²⁺ with different cations (2 mM), λ_{ex} = 320 nm, λ_{em} = 460 nm; black, competing ions; red, competing ions + Zn²⁺. (A) only 1, (B) Mg²⁺, (C) Na⁺, (D) Ca²⁺, (E) Co²⁺, (F) Cu⁺, (G) Cu²⁺, (H) Eu³⁺, (I) Fe³⁺, (J) Hg²⁺, (K) Mn²⁺, (L) Nd³⁺, (M) NH₄⁺, (N) Ni²⁺, (O) Sr²⁺, (P) K⁺, (Q) Cd²⁺, and (R) Ag⁺. (b) Fluorescence of 1 in a CH₃CN solution upon the addition of Zn²⁺ and K⁺. (black) Only 1; (red) 1 with K⁺ (first 0.8 mM) and Zn²⁺ (0.2 mM); (blue) 1 with Zn²⁺ (0.2 mM); (cyan) 1 with Zn²⁺ (0.2 mM, first) and K⁺ (0.8 mM).

the Supporting Information). So, the sequence of adding K⁺ and Zn²⁺ ions to the solution of 1 was investigated first to explore whether it can lead to different fluorescence spectra. As shown in Figure 3b, upon the addition of Zn²⁺ (0.2 mM) to the mixture of 1 and K⁺ ion, i.e., “off-state”, the emission band at 460 nm did not appear and the fluorescence spectra were similar to that of free 1 (see Figures 3b and S6b in the Supporting Information). However, upon the addition of Zn²⁺ to the mixture of 1 and the above-mentioned other tested metal

ions, the emission band at 460 nm due to the 1-Zn²⁺ complex, i.e., “on-state”, stood still unaffected (see Figure 3a). Conversely, upon the addition of K⁺ ions to the mixture of 1 and Zn²⁺ ions, the emission band at 396 nm appeared again accompanied with the disappearance of the emission band at 460 nm (see Figures 3b and S7 in the Supporting Information). Also, the fluorescence quantum yield of a 1-Zn²⁺ solution was decreased from 0.75 to 0.19¹⁸ when K⁺ was added to it. It is interesting to note that the fluorescence intensity of 1 was also affected by the addition sequence of Zn²⁺ and K⁺. The fluorescent quenching of 1 due to the addition of Zn²⁺ (0.2 mM) and then K⁺ (0.8 mM) was much greater than that due to the addition of K⁺ (0.8 mM) and then Zn²⁺ (0.2 mM; see Figures 3b and S7 in the Supporting Information). Thus, we can conclude that the different sequences of the addition of Zn²⁺ and K⁺ ions to the solution of 1 in CH₃CN induced different emission changes, permitting this complex could effectively act as an INHIBIT molecular device of logic gate and on–off switch.

Then, upon the addition of K⁺ ions to the solution of 1-Zn²⁺, the changes of the UV–vis spectra were similar to its emission spectra, which could revive the original absorption spectra of 1 (see Figure S8 in the Supporting Information). The addition of Zn²⁺ ions to the solution of 1-K⁺ led to a decrease in the intensity at 365 nm (see Figure S9 in the Supporting Information), while the addition of Zn²⁺/K⁺ ions to the solution of 1 with different sequences could induce different absorption spectral changes, indicating that 1 can obviously act as a logic device as well. The fluorescence properties of 1 were also studied in a 9:1 CH₃CN/H₂O solution, and the results showed changes of fluorescence very similar to those in an acetonitrile solution (see Figures S10 and S11 in the Supporting Information).

Theoretical Studies. The time-dependent DFT by the Gaussian 03¹⁶ program was applied to make clear the changes in the electronic properties. As we know, the highest occupied molecular orbital (HOMO)–lowest unoccupied molecular orbital (LUMO) gap and the electronic distributions may be used to clarify the changes in the fluorescent properties with metal cation coordination and detect the ratiometric response to metal cations.²⁰ In the case of free 1 (see Figure 4a), π electrons on the HOMO mainly focus on the pyridyl units,

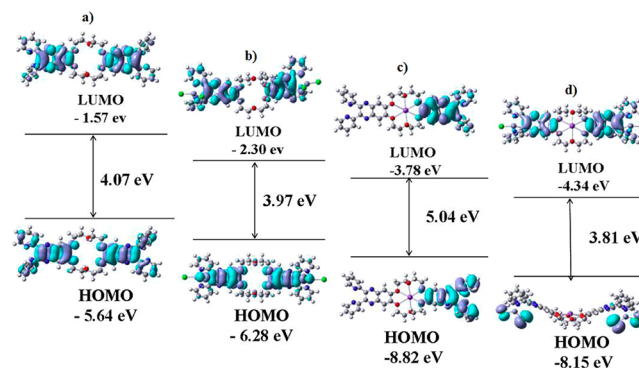
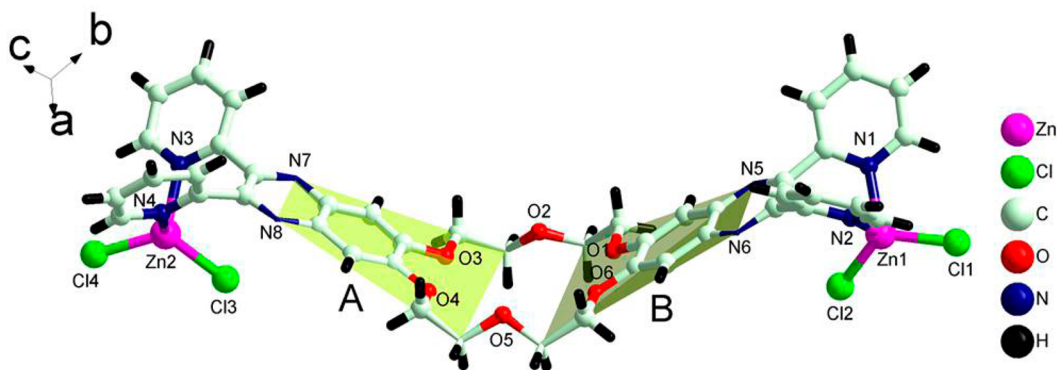
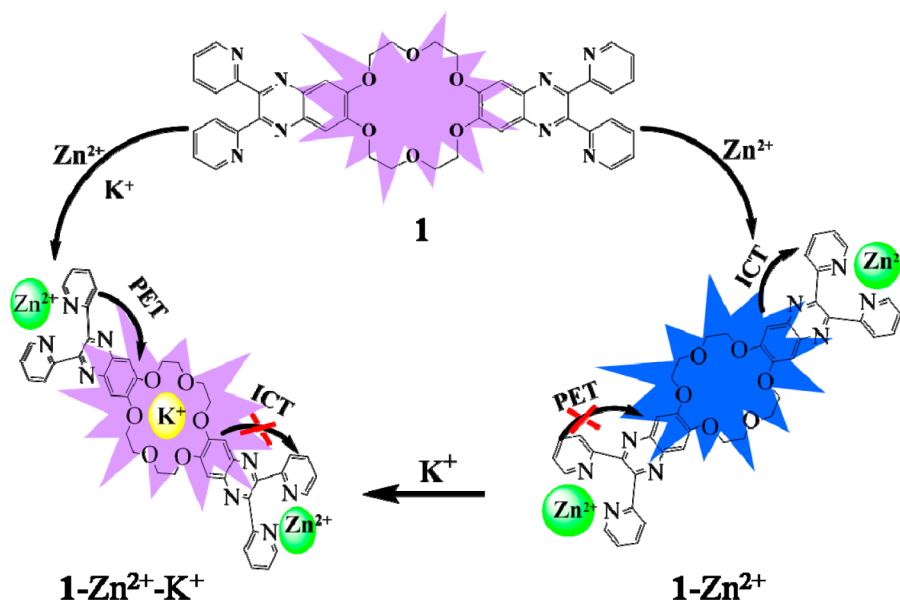


Figure 4. HOMO–LUMO energy gaps for respective compounds and interfacial plots of the orbitals: (a) free 1; (b) 1-Zn²⁺ complex; (c) 1-K⁺ complex; (d) 1-K⁺/Zn²⁺ complex. Gray, red, and blue atoms of the molecular frameworks indicate the C, O, N, and metal atoms, respectively. Gray and deep-cyan parts on the interfacial plots refer to the different phases of the molecular wave functions, for which the isovalue is 0.02 au.

Chart 1

Figure 5. View of the coordination geometry of Zn^{2+} in 1-Zn .

whereas those on the LUMO mainly focus on quinoxaline. In the presence of Zn^{2+} ions, upon Zn^{2+} binding with the N atom of the pyridyl units, the energy levels of both HOMO and LUMO are lower than those of free **1**. The π electrons that focus on the LUMO of the 1:2 complex (1-Zn^{2+}) are distributed on the pyridyl moiety, which makes the 1-Zn^{2+} complex stabilize the π electrons on the pyridyl moieties. Also, the decreasing energy in the LUMO level is more significant than that of the HOMO, indicating that the LUMO is more stabilized. This results strongly proved the ICT from the quinoxaline to the pyridyl moieties, which leads to a red shift in the fluorescence spectra by stabilizing the energy levels of LUMO upon interacting pyridine units with zinc ions (see Figure 4b).²¹

In the presence of K^+ ions, the distribution of the π electrons on HOMO and LUMO is similar to the free **1**, which is mainly located at pyridyl moieties and quinoxaline, respectively (see Figure 4c). However, when both K^+ and Zn^{2+} ions are present, the distribution of the π electrons on HOMO and LUMO is obviously unlike that of the 1-Zn^{2+} complex (see Figure 4d). So, the presence of K^+ ions blocked the ICT processes between **1** and Zn^{2+} ions^{4e,22} and caused the PET processes. Thus, the addition of Zn^{2+} ions to the mixture of 1-K^+ only decreased the fluorescence intensity of the band at 396 nm without a red shift

(see Figure S6 in the SI). As illustrated in Figure 4d, the π electrons on the HOMO of the $1\text{-K}^+/\text{Zn}^{2+}$ complex are only distributed on the chloride anions of zinc chloride, but the π electrons on the LUMO are distributed on the quinoxaline. The energies of both the HOMO and LUMO of the $1\text{-K}^+/\text{Zn}^{2+}$ complex are lower than those of the free **1** and 1-K^+ complex. More importantly, the energy of the $1\text{-K}^+/\text{Zn}^{2+}$ complex is lower than that of the 1-Zn^{2+} complex, indicating that the $1\text{-K}^+/\text{Zn}^{2+}$ complex strongly promotes the PET process through stabilization of the LUMO by the coordination of K^+ and Zn^{2+} with the crown and pyridyl moieties, respectively (Chart 1).

Crystal Structures. We can see that **1** and Zn^{2+} form a structure with 1:2 stoichiometry (see Figure 5). Single-crystal X-ray determination reveals that compound 1-Zn crystallizes in the triclinic space group $P\bar{1}$. Both zinc centers adopt distorted tetrahedral geometry through bidentate coordination of **1**. Each Zn^{2+} ion is coordinated by two N atoms of pyridyl and two Cl^- ions, with the Zn–N bond lengths ranging from 2.045 to 2.071 Å. As shown in Figure 1, the dihedral angle between plane A (formed by N7, N8, O3, O4, etc.) and plane B (formed by N5, N6, O1, O6, etc.) is 54.10° .

Logic Gates and an Off–On–Off Switch Based on **1 with Zn^{2+} and K^+ as the Inputs.** It has been reported that fluorescence sensors can act as logic gates, but the inputs of the

logic gates are mainly toxic heavy metals like Cu^{2+} , Hg^{2+} , and so on.^{6,22} As shown in Figure 6, when only Zn^{2+} was added to the

Input (K^+)	Input (Zn^{2+})	Output (396 nm)	Output (460 nm)
0	0	1	0
1	0	1	0
0	1	0	1
1	1	1	0

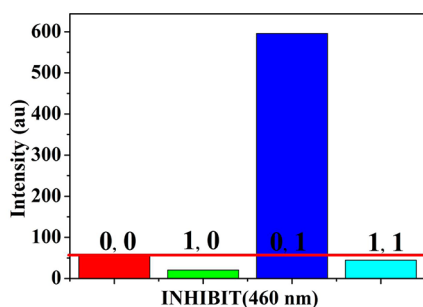


Figure 6. Truth table (top) and the combinatorial logic scheme (bottom) of INHIBIT logic operations.

solution of **1**, the emission spectra were red-shifted about 64 nm from 396 to 460 nm. However, upon the addition of both K^+ and Zn^{2+} with different sequences, the fluorescence spectra of **1** were changed differently. Furthermore, the effect of Zn^{2+} and K^+ on the fluorescence of **1** can be used in a more advanced molecular device, such as logic gates. A two-input INHIBIT logic gate was successfully mimicked for **1**. As shown in Figure 6, K^+ (input 1, 0.8 mM) and Zn^{2+} (input 2, 0.2 mM) were used as inputs; the emission band at 460 nm was taken as the output in this system. The emission intensity at 460 nm was distinctly high only when the inputs were in a (0, 1) sequence, while the output was low when inputs were (1, 0). Thus, a two-input INHIBIT logic gate was fabricated by using Zn^{2+} and K^+ as inputs and taking I_{460} as the output. Moreover, when K^+ was added to the mixture of a **1**- Zn^{2+} solution, the emission band at 460 nm was decreased and recovered the original emission states (see Figure S7 in the Supporting Information); meanwhile, the visible emission color of the **1**- Zn^{2+} complex solution was gradually disappearing upon the addition of K^+ (see Figure S12 in the Supporting Information). As a result, Zn^{2+} (first) and K^+ (last) fabricated an off–on–off switch.

CONCLUSION

A new chemosensor, **1**, in which the 2,3-bis(pyridin-2-yl)quinoxaline group was incorporated with a [2,4]dibenzo-18-crown-6 core to form a ditopic environment and create two different coordination modes for binding different kinds of metal ions, has been well designed. We demonstrated that the emission states and electronic distribution of **1** could be conveniently controlled by the addition order of Zn^{2+} and K^+ . These results confirmed that **1** may be performed as a molecular device of a novel INHIBIT logic gate and an off–on–off molecular switch. Further studies are underway in our laboratory.

ASSOCIATED CONTENT

Supporting Information

Experimental procedures, characterization data for the synthesis, crystal data, and calculated information, and X-ray structural data for CCDC 849766 and 849767 in CIF format. This material is available free of charge via the Internet at <http://pubs.acs.org>.

AUTHOR INFORMATION

Corresponding Author

*E-mail: buxh@nankai.edu.cn. Tel: +86-22-23502809. Fax: +86-22-23502458.

Notes

The authors declare no competing financial interest.

ACKNOWLEDGMENTS

This work was supported by the 973 Program (Grant 2012CB821700), NSFC (Grants 21031002 and 51073079), and the NSF of Tianjin, China (Grant 10JCZDJC22100).

REFERENCES

- (1) For example, see: (a) Chimienti, F.; Devergnas, S.; Pattou, F.; Schuit, F.; Garcia, C. R.; Vandewalle, B.; Kerr-Conte, J.; Van, L. L.; Grunwald, D.; Favier, A.; Seve, M. *J. Cell. Sci.* **2006**, *119*, 4199. (b) Frederickson, C. J.; Koh, J. Y.; Bush, A. I. *Nat. Rev. Neurosci.* **2005**, *6*, 449. (c) Costello, L. C.; Franklin, R. B.; Feng, P.; Tan, M.; Bagasra, O. *Cancer, Causes Control* **2005**, *16*, 901.
- (2) For example, see: (a) Xu, Z.; Yoon, J.; Spring, D. R. *Chem. Soc. Rev.* **2010**, *39*, 1996. (b) Nolan, E. M.; Lippard, S. J. *Acc. Chem. Res.* **2009**, *42*, 193. (c) Que, E. L.; Domaille, D. W.; Chang, C. J. *Chem. Rev.* **2008**, *108*, 1517. (d) Komatsu, K.; Urano, Y.; Kojima, H.; Nagano, T. *J. Am. Chem. Soc.* **2007**, *129*, 13447.
- (3) (a) Maruyama, S.; Kikuchi, K.; Hirano, T.; Urano, Y.; Nagano, T. *J. Am. Chem. Soc.* **2002**, *124*, 10650. (b) Kiyose, K.; Kojima, H.; Urano, Y.; Nagano, T. *J. Am. Chem. Soc.* **2006**, *128*, 6548. (c) Woodroffe, C. C.; Lippard, S. J. *J. Am. Chem. Soc.* **2003**, *125*, 11458. (d) Taki, M.; Wolford, J. L.; O'Halloran, T. V. *J. Am. Chem. Soc.* **2004**, *126*, 712. (e) Henary, M. M.; Wu, Y.; Fahrni, C. J. *Chem.—Eur. J.* **2004**, *10*, 3015. (f) Mei, Y. J.; Bentley, P. A. *Bioorg. Med. Chem. Lett.* **2006**, *16*, 3131. (g) Jiang, P.; Guo, Z. *Coord. Chem. Rev.* **2004**, *248*, 205. (h) Kikuchi, K.; Komatsu, K.; Nagano, T. *Curr. Opin. Chem. Biol.* **2004**, *8*, 182. (i) Lim, N. C.; Freake, H. C.; Brückner, C. *Chem.—Eur. J.* **2005**, *11*, 38. (j) Carol, P.; Sreejith, S.; Ajayaghosh, A. *Chem.—Asian J.* **2007**, *2*, 338. (k) Atilgan, S.; Ozdemir, T.; Akkaya, E. U. *Org. Lett.* **2008**, *10*, 4065. (l) Wu, Y.; Peng, X.; Guo, B.; Fan, J.; Zhang, Z.; Wang, J.; Cui, A.; Gao, Y. *Org. Biomol. Chem.* **2005**, *3*, 1387. (m) Koutaka, H.; Kosuge, J.; Fukasaku, N.; Hirano, T.; Kikuchi, K.; Urano, Y.; Kojima, H.; Nagano, T. *Chem. Pharm. Bull.* **2004**, *52*, 700. (n) Tufan, B.; Akkaya, E. U. *Org. Lett.* **2002**, *4*, 2857.
- (4) (a) de Silva, A. P.; Gunaratne, H. Q. N.; McCoy, C. P. *Nature* **1993**, *364*, 42. (b) Szacilowski, K. *Chem. Rev.* **2008**, *108*, 3481. (c) de Silva, A. P.; Uchiyama, S.; Vance, T. P.; Wannalerse, B. *Coord. Chem. Rev.* **2007**, *251*, 1623. (d) Guliyev, R.; Ozturk, S.; Kostereli, Z.; Akkaya, E. U. *Angew. Chem., Int. Ed.* **2011**, *50*, 9826. (e) Bozdemir, O. B.; Guliyev, R.; Buyukcikir, O.; Selcuk, S.; Kolem, S.; Gulcihan, G.; Nalbantoglu, T.; Boyaci, H.; Akkaya, E. U. *J. Am. Chem. Soc.* **2010**, *132*, 8029.
- (5) (a) Rinaudo, K.; Bleris, L.; Maddamsetti, R.; Subramanian, S.; Weiss, R.; Beneson, Y. *Nat. Biotechnol.* **2007**, *25*, 795. (b) Li, A. F.; Jiang, Q. Q.; He, W. B.; Jiang, Y. B. *Chem.—Eur. J.* **2010**, *16*, 5794. (c) Ruiters, G. D.; Boom, M. E. V. D. *Acc. Chem. Res.* **2011**, *44*, 563.
- (6) (a) Liu, Y.; Li, M. Y.; Zhao, Q.; Wu, H. Z.; Huang, K.; Li, F. Y. *Inorg. Chem.* **2011**, *50*, 5969. (b) Huang, W. T.; Shi, Y.; Xie, W. Y.; Luo, H. Q.; Li, N. B. *Chem. Commun.* **2011**, *47*, 7800. (c) Manoj, K.; Rajesh, K.; Vandana, B. *Chem. Commun.* **2009**, 7384. (d) Chen, S. Y.;

- Yang, Y. H.; Wu, Y.; Tian, H.; Zhu, W. H. *J. Mater. Chem.* **2012**, *22*, 5486.
- (7) (a) Khan, F. A.; Parasuraman, K.; Sadhu, K. K. *Chem. Commun.* **2009**, 2399. (b) Guo, Z. Q.; Zhu, W. H.; Shen, L. J.; Tian, H. *Angew. Chem., Int. Ed.* **2007**, *46*, 5549. (c) Petitjean, A.; Kyritsakas, N.; Lehn, J. M. *Chem.—Eur. J.* **2005**, *11*, 6818.
- (8) (a) Motornov, M. M.; Zhou, J.; Pita, M.; Gopishetty, V.; Tokarev, I.; Katz, E.; Minko, S. *Nano Lett.* **2008**, *8*, 2993. (b) Komatsu, H.; Matsumoto, S.; Tamaru, S. I.; Kaneko, K.; Ikeda, M.; Hamachi, I. *J. Am. Chem. Soc.* **2009**, *131*, 5580. (c) Shlyahovsky, B.; Li, Y.; Lioubashevski, O.; Elbaz, J.; Willner, I. *ACS Nano* **2009**, *3*, 1831. (d) He, X. M.; Yam, V. W. W. *Org. Lett.* **2011**, *13*, 9.
- (9) (a) Valeur, B.; Leray, I. *Coord. Chem. Rev.* **2000**, *205*, 3. (b) Valeur, B.; Leray, I. *Inorg. Chem. Acta* **2007**, *360*, 765. (c) Yuan, M.; Zhou, W.; Liu, X.; Zhu, M.; Li, J.; Yin, X.; Zheng, H.; Zuo, Z.; Ouyang, C.; Liu, H.; Li, Y.; Zhu, D. *J. Org. Chem.* **2008**, *73*, 5008. (d) Xu, Z. C.; Liu, X.; Pan, J.; Spring, D. R. *Chem. Commun.* **2012**, 48, 4764.
- (10) (a) Baruah, M.; Qin, W. W.; Vallée, R. A. L.; Beljonne, D.; Rohand, T.; Dehaen, W.; Boens, N. *Org. Lett.* **2005**, *7*, 20. (b) Deck, C.; Meister, A.; Hause, G.; Baro, A.; Laschat, S. *Chem.—Eur. J.* **2010**, *16*, 6326.
- (11) (a) Kaur, N.; Singh, N.; Cairns, D.; Callan, J. F. *Org. Lett.* **2009**, *11*, 2229. (b) Chaudhry, A. F.; Mandal, S.; Hardcastle, K. I.; Fahrni, C. J. *Chem. Sci.* **2011**, *2*, 1016. (c) Ou, S. J.; Lin, Z. H.; Duan, C. Y.; Zhang, H. T.; Bai, Z. P. *Chem. Commun.* **2006**, 4392. (d) Ashokkumar, P.; Ramakrishnan, T. V.; Ramamurthy, P. *J. Phys. Chem. A* **2011**, *115*, 14292. (e) Lo, H. S.; Yip, S. K.; Wong, K. M. C.; Zhu, N. Y.; Yam, V. W. W. *Organometallics* **2006**, *25*, 3537.
- (12) (a) Bu, X. H.; Liu, H.; Du, M.; Wong, K. M. C.; Yam, V. W. W.; Shionoya, M. *Inorg. Chem.* **2001**, *40*, 4143. (b) Dennis, A. E.; Smith, R. C. *Chem. Commun.* **2007**, 4641. (c) Felton, C. E.; Harding, L. P.; Jones, J. E.; Kariuki, B. M.; Pope, S. J. A.; Rice, C. R. *Chem. Commun.* **2008**, 6185. (d) Zhao, Q.; Li, R. F.; Xing, S. K.; Liu, X. M.; Hu, T. L.; Bu, X. H. *Inorg. Chem.* **2011**, *50*, 10041.
- (13) Duggan, S. A.; Fallon, G.; Langford, S. J.; Laau, V. L.; Satchell, J. F.; Paddon-Row, M. N. *J. Org. Chem.* **2001**, *66*, 4419.
- (14) SAINT Software Reference Manual; Bruker AXS: Madison, WI, 1998.
- (15) Sheldrick, G. M. *SHELXTL NT: Program for Solution and Refinement of Crystal Structures*, version 5.1; University of Göttingen: Göttingen, Germany, 1997.
- (16) Frisch, M. J.; Trucks, G. W.; Schlegel, H. B.; Scuseria, G. E.; Robb, M. A.; Cheeseman, J. R.; Montgomery, J. A.; Vreven, J. T.; Kudin, K. N.; Burant, J. C.; Millam, J. M.; Iyengar, S. S.; Tomasi, J.; Barone, V.; Mennucci, B.; Cossi, M.; Scalmani, G.; Rega, N.; Petersson, G. A.; Nakatsuji, H.; Hada, M.; Ehara, M.; Toyota, K.; Fukuda, R.; Hasegawa, J.; Ishida, M.; Nakajima, T.; Honda, Y.; Kitao, O.; Nakai, H.; Klene, M.; Li, X.; Knox, J. E.; Hratchian, H. P.; Cross, J. B.; Adamo, C.; Jaramillo, J.; Gomperts, R.; Stratmann, R. E.; Yazyev, O.; Austin, A. J.; Cammi, R.; Pomelli, C.; Ochterski, J. W.; Ayala, P. Y.; Morokuma, K.; Voth, G. A.; Salvador, P.; Dannenberg, J. J.; Zakrzewski, V. G.; Dapprich, S.; Daniels, A. D.; Strain, M. C.; Farkas, O.; Malick, D. K.; Rabuck, A. D.; Raghavachari, K. J.; Foresman, B.; Ortiz, J. V.; Cui, Q.; Baboul, A. G.; Clifford, S.; Cioslowski, J.; Stefanov, B. B.; Liu, G.; Liashenko, A.; Piskorz, P.; Komaromi, I.; Martin, R. L.; Fox, D. J.; Keith, T.; Al-Laham, M. A.; Peng, C. Y.; Nanayakkara, A.; Challacombe, M. P.; Gill, M. W.; Johnson, B.; Chen, W.; Wong, M. W.; Gonzalez, C.; Pople, J. A. *Gaussian03*; Gaussian, Inc.: Pittsburgh, PA, 2003.
- (17) (a) Choi, C. M.; Lee, J. H.; Choi, Y. H.; Kim, H. J.; Kim, N. J. *J. Phys. Chem. A* **2009**, *113*, 8343. (b) Choi, C. M.; Lee, J. H.; Choi, Y. H.; Kim, H. J.; Kim, N. J.; Heo, J. J. *J. Phys. Chem. A* **2010**, *114*, 11167. (c) Inokuchi, Y.; Boyarkin, O. V.; Kusaka, R.; Haino, T.; Ebata, T.; Rizzo, T. R. *J. Am. Chem. Soc.* **2011**, *133*, 12256.
- (18) Casey, K. G.; Quitevis, E. L. *J. Phys. Chem.* **1988**, *92*, 6590.
- (19) Sabatini, A.; Vacca, A.; Gans, P. *Coord. Chem. Rev.* **1992**, *120*, 389.
- (20) McGrier, J.; Bunz, P. L.; Bunz, U. H. F. *Acc. Chem. Res.* **2010**, *43*, 397.
- (21) (a) Shiraishi, Y.; Ichimura, C.; Sumiya, S.; Hirai, T. *Chem.—Eur. J.* **2011**, *17*, 8324. (b) Zhang, L.; Clark, R. J.; Zhu, L. *Chem.—Eur. J.* **2008**, *14*, 2894. (c) Younes, A. H.; Zhang, L.; Clark, R. J.; Zhu, L. *J. Org. Chem.* **2009**, *74*, 8761.
- (22) (a) Nishimura, G.; Ishizumi, K.; Shiraishi, Y.; Hirai, T. *J. Phys. Chem. B* **2006**, *110*, 21596. (b) Kumar, S.; Singh, P.; Kaur, S. *Tetrahedron* **2007**, *63*, 11724. (c) Dhir, A.; Bhalla, V.; Kumar, M. *Org. Lett.* **2008**, *10*, 21.